

A beam position monitor for the diagnostic line in MEBT2 of J-PARC linac

A Miura, J Tamura and Y Kawane

J-PARC Center, Japan Atomic Energy Agency, 2-4, Shirakata-Shirane, Tokai, Ibaraki, 319-1195, JAPAN

E-mail: akihiko.miura@j-parc.jp

Abstract. In the linac of the Japan Proton Accelerator Research Complex (J-PARC), the neutral hydrogen (H^0) beam from the negative hydrogen ion (H^-) beam is one of key issues in mitigating beam losses. To diagnose H^0 particles, we installed a set of beam-bump magnets to generate a chicane orbit of the H^- beam. The beam position monitors (BPMs) in the beam line are used for orbit correction to maintain the beam displacement within 2.0 mm from the duct center. To measure the beam displacement under different drive currents of the beam-bump magnets, a new wide-range BPM was designed and manufactured to evaluate the horizontal beam position by using a correction function to compensate for non-linearity. We also employed the beam profile monitor (WSM: wire scanner monitor) to measure the H^- beam profile, which helped us to compare the beam position measurements. In this paper, the design and the performance of the wide-range BPM are described. In addition, we present a comparison of the beam position measured by the BPM and the WSM.

1. Introduction

In the Japan Proton Accelerator Research Complex (J-PARC) linac, a diagnostics beam line incorporating a beam bump was installed in the medium energy beam transport (MEBT2) part, between the section of a separation-type drift tube linac (SDTL) and an annular-ring coupled structure linac (ACS). The diagnostics to measure beam displacement and to detect H^0 particles were prepared for the diagnostics line in the summer of 2015 [1]. The diagnostics line comprises four beam-bump magnets which are structurally identical to produce a chicane orbit in the horizontal plane, as depicted in Figure 1 and 2. The transverse profile monitor (WSM: wire scanner monitor), located in the beam line is used to measure the intensity distribution of both the H^+ and H^0 particles by using a carbon plate mounted on a sensor head of the WSM. In addition, the performances of the beam-bump magnets and their power supplies were evaluated by measuring beam displacements by using a beam position monitor (BPM). We use a rectangular beam duct with dimensions of 100 mm horizontally and 40 mm vertically for a maximum beam displacement of 30 mm horizontal to avoid a scraping of the beam core.

More than 40 BPMs have already been fabricated and installed in the MEBT2 and ACS beam line [2], and they are used for standard orbit-correction procedures. Following the J-PARC tuning policy, the beam orbit must be located within 2.0 mm of the duct center, the measurement accuracy of the beam-line BPMs are required to be within 5.0 mm from the duct center. We designed and fabricated a wide-range BPM beam pickup considering the aperture and the beam orbit variations.



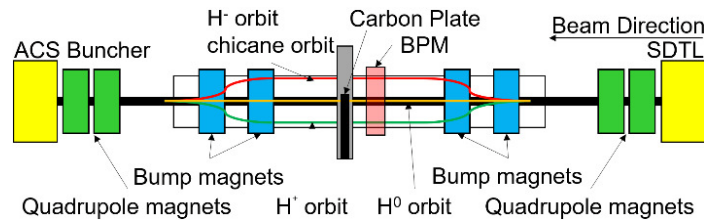


Figure 1. Device Location in MEBT2 Diagnostics Line.

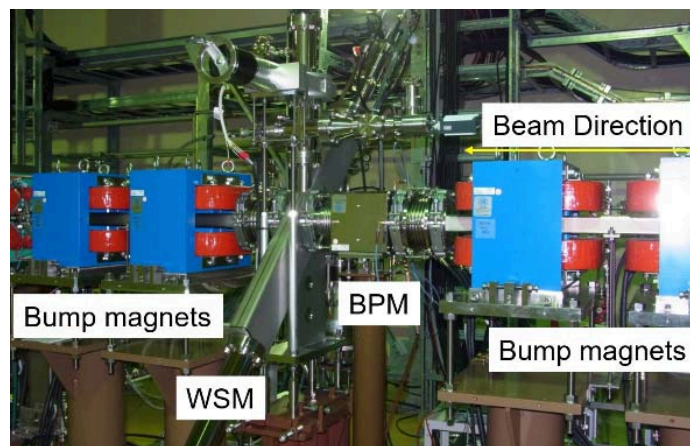


Figure 2. Installation of Bump Magnet and Diagnostics in MEBT2 Diagnostic Line.

After installation of the newly fabricated BPM in diagnostics line, the beam displacements were evaluated by comparing the magnet supply currents with the BPMs. The measured beam positions were compared with the beam center positions found in the beam profile obtained using the WSM. This paper describes the design the BPM, its calibration and evaluation results.

2. Design of the Beam Position Monitor

2.1. Design of the BPM pickup

An alternating current signal is induced on the electrode, coupled at radio frequencies (RF) and is four pick-up electrodes are installed crosswise in the beam duct and the difference in the signals of the counter-facing electrodes in the center-of-mass of the beam.

For low- β beams, the three dimensional (3D) Laplace equation must be used when the beam current modulation wavelength is comparable to the aperture. The position sensitivity of pairs of BPM pickup electrodes was estimated using Equations (1) and (2) and the Lorentz factor. Image charges in the form of logarithmic ratio in dB are given by the following functions [3]:

$$\left(\frac{I_{WR}}{I_{WL}}\right) = \frac{160}{\ln(10)} (1 + G) \frac{\sin(\phi/2) x}{\phi b} + O(x^2), \quad (1)$$

where G is given as:

$$G = 0.139 \left(\frac{\omega b}{\beta \gamma c}\right)^2 - 0.0145 \left(\frac{\omega b}{\beta \gamma c}\right)^3. \quad (2)$$

Here, ϕ is the electrode opening angle, b is the radius of the beam duct, x is the beam position, ω is the angular frequency, $O(x^2)$ denotes the higher-order terms in x , c is the velocity of light, and γ is the Lorentz factor.

In our application a stripline type electrode was selected for this diagnostics BPM, as it could be better matched operating at the acceleration frequency compared to the button-style BPM electrodes owing their stray capacitances [4].

Figure 3 shows a drawing of the BPM. A large aperture with an inner diameter of 120 mm was selected to ensure the measurement of displacement [1]. The signal induced on a stripline by the beam charge is proportional to the distance between the electrode and the beam, as well as to the beam intensity, and it further depends on the dimensions, for example, length and width, of the stripline. If the characteristic impedance at both the upstream and the downstream ports is equal to the characteristic impedance of the stripline (here: $Z_0 = 50 \Omega$), the voltage induced at the upstream port of a stripline electrode of length (l) is given as follows [5] :

$$V(\omega) = \frac{\phi Z_0}{2\pi} I_b(\omega) \sin \left[\frac{\omega l}{2c} \left(\frac{1}{\beta_s} - \frac{1}{\beta_b} \right) \right], \quad (3)$$

where ϕ represents the opening angle of the stripline electrode (Figure 3); $I_b(\omega)$ the beam spectrum, here detected at the RF acceleration frequency of 324 MHz, β_s the relative velocity of the signal on the stripline electrode; and β_b the relative velocity of the beam. By using Equation (3), we optimized the electrode length to achieve the maximum output signal voltage at our operation frequency, which is 155 mm for our beam energy of 191 MeV ($\beta_b = 0.56$).

The width of the stripline was determined based on its characteristic impedance, and it was found to be 50Ω to match the impedance of the signal cable. To determine the width of the stripline, we calculated the characteristic impedance of the stripline by using the cross-sectional distribution of the electrical field generated by the potential difference between the electrode and the beam duct [6]. The characteristic impedance was then calculated based on a numerical, two-dimensional Poisson equation calculation code called ‘‘Poisson Super Fish’’ [7]. An example of the calculated electrical field is shown in Figure 4. In the narrow space, which is the gap between the stripline and the body, there is ceramic insulation, and high-electrical-field regions can be observed. After varying the width of the stripline as a parameter in those two-dimensional calculations, we fabricated prototype pickups, and finally set the width to 34.40 mm.

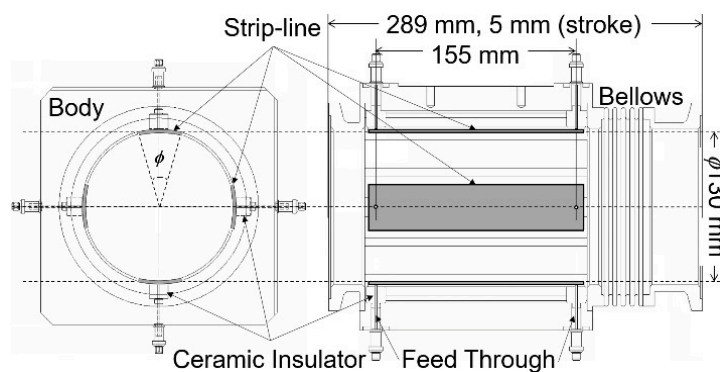


Figure 3. Drawing of BPM for diagnostic line in MEBT2 of J-PARC linac.

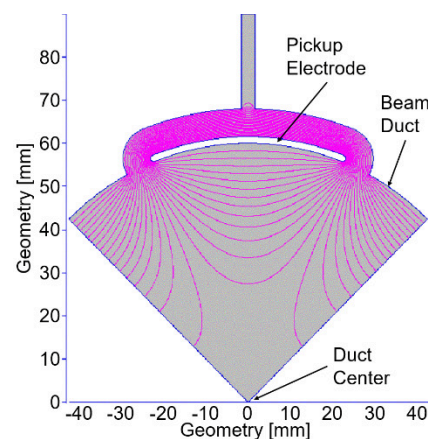


Figure 4. 2D Simulation results of electrical field in a cross section around one electrode pickup.

2.2. Signal processing

The logarithmic ratio method of signal processing was selected because of its robustness and wide dynamic range. The output signal from the logarithmic amplifier was low-pass-filtered for noise reduction. The beam position obtained by the logarithmic processing is as follows [3]:

$$x = \frac{1}{S} \cdot (\log V_R - \log V_L) = \frac{1}{S_x} \cdot \log \frac{V_R}{V_L} \propto \frac{1}{S_x} \cdot V_{out} \quad (4)$$

Position sensitivity given by S in [dB/mm], and V_R and V_L are induced signal voltages [V] of the right and the left electrodes, respectively. Sensitivity is described below in terms of stripline width W ,

$$S = \frac{160}{\ln 10} \times \frac{\sin(\phi/2)}{\phi} \times \frac{1}{r} = \frac{160}{\ln 10} \times \frac{W}{2\phi} \times \frac{1}{r}. \quad (5)$$

For calculation of the beam position, for example, the vertical position X [mm] is given below using Equation (4),

$$X = \frac{1}{S} \cdot 20 \log_{10} \left(\frac{V_R}{V_L} \right). \quad (6)$$

3. Calibration

We measured the electrical center of the BPM by using a simulated beam signal induced on a stretched wire calibration bench, as in Figure 5. To compare the position of the physical wire and its reconstructed position obtained from the electrical BPM readout, the following scheme was used in the calibration bench.

- The wire was scanned through the transverse cross section of the BPM, horizontally and vertically, by applying a 324 MHz RF stimulus signal.

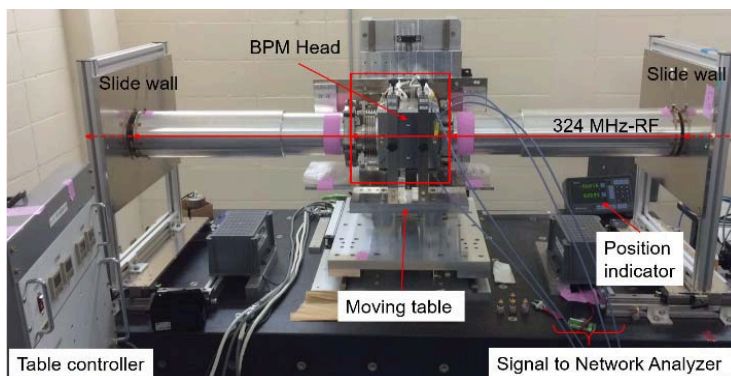


Figure 5. Overview of calibration bench for BPM.

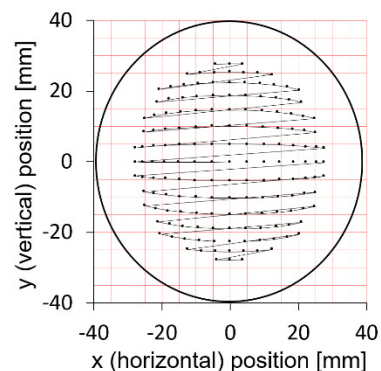


Figure 6. Mapping of BPM position characteristics moving wire.

- The induced electrode signals were processed with logarithmic amplifiers on a 50 Ω load. The ratios of the demodulated output signals between the right and the left, and the top and the bottom electrodes give the horizontal and vertical measured beam positions, respectively.
- We interpolated (curve fitting) the acquired position values. As shown in Figure 6, for large displacements of the wire (especially under 45° of the x-y coordinates), the non-linear effects become stronger. For correction, a fitting function must be derived. Moreover, fitting functions are required for displacement than 20 mm. In addition, this calibration method excited with either pulses or high-frequency sinusoidal currents, the EM wave represents the principal (TEM) mode in a coaxial transmission line. Thus, the stretched-wire method is unsuitable for the simulation of slow particle beams in high frequency diagnostic devices. Assuming position displacement by using the applicable fitting function comprising a fourth-order polynomials, we extrapolated the calibration results to the obtained BPM mapping (Figure 6).

Figure 6 shows the relationship between the mechanical and the electrical position. The red points represent the position of the wire, scanned throughout the BPM aperture. Red dots indicate the wire

position on a 1.0-mm square grid, and the black ones are the obtained wire positions. The horizontal (X) and vertical position values (Y) were measured directly by the logarithmic amplifier module. For relativistic beams, we considered the fitting function to be adaptable in a region of radius 25.0 mm.

As the fitting function, we derived a fourth-order polynomial for the x and y :

$$x = -3.594e-8m^4 - 1.608e-8m^3n - 6.455e-8m^2n^2 + 5.623e-7mn^3 + 7.265e-9n^4 - 5.518e-5m^3 + 1.819e-6m^2n + 1.970e-4mn^2 + 5.375e-6n^3 + 3.305e-5m^2 - 6.008e-5mn + 1.970e-4n^2 + 9.561e-1m + 3.305e-5n + 3.498e-3 \quad (7)$$

$$y = -1.566e-8e-8m^4 - 7.372e-8m^3n + 1.785e-7m^2n^2 - 1.056e-7mn^3 + 2.165e-8n^4 - 2.635e-7m^3 + 1.845e-4m^2n + 5.204e-6mn^2 - 5.057e-5n^3 - 1.405e-6m^2 + 6.896e-5mn - 7.083e-5n^2 + 2.343e-3m + 9.572e-1n + 0.209 \quad (8)$$

where m and n are the position values reported by the logarithmic amplifier signals. m is the horizontal position and n is the vertical position. We implemented these fourth-order fitting functions, corrected the BPM pickup non-linearity, and reported the resulting beam position.

4. Orbit-Shift Evaluation by Transverse Profile

We used a WSM to evaluate beam displacement from the transverse beam profile. A tungsten wire of diameter 0.03 mm was used to measure the beam profile. The WSM is a suitable device to evaluate the beam displacement, because the scan range of WSM is strictly maintained. The results of the beam profile measurement with several current sets of the beam-bump magnet are summarized in Figure 7. The beam profile peaks corresponding to 10-A intervals of the magnet can be observed 7.5-mm apart.

5. Measurement Results

The beam positions acquired by the WSM measurements are plotted in Figure 8 along with the acquired BPM data for comparison. The WSM measurement shows a high linearity, even for large beam displacements. The measured beam position of WSM and BPM differs slightly, particularly at large beam displacements. One reason is the linear fitting function only considers distance less than 20 mm, so the errors depend upon the distance from the center. The gradient of the fitting function of BSM is about 7-8 % smaller than that of WSM. It is considered to be an error of the value of sensitivity described by Equation (6). The sensitivity is defined by the geometrical parameters, if a negligible error exists, the measurement errors extend linearly. Usually, the fitting function is applied for a range of 5.0 mm from the beam center. However, this function was extended to consider larger

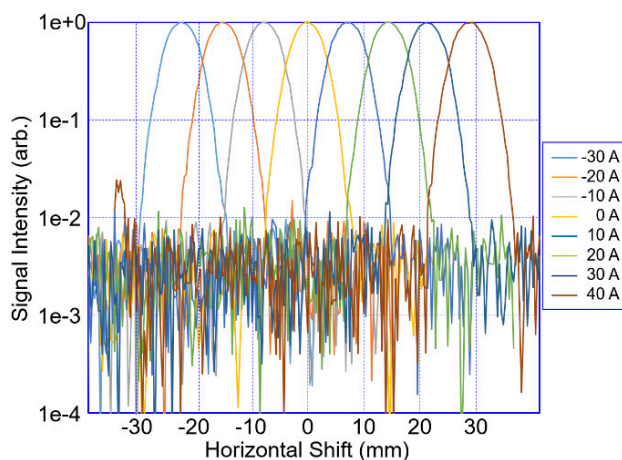


Figure 7. Beam profile measurement results with several current-sets.

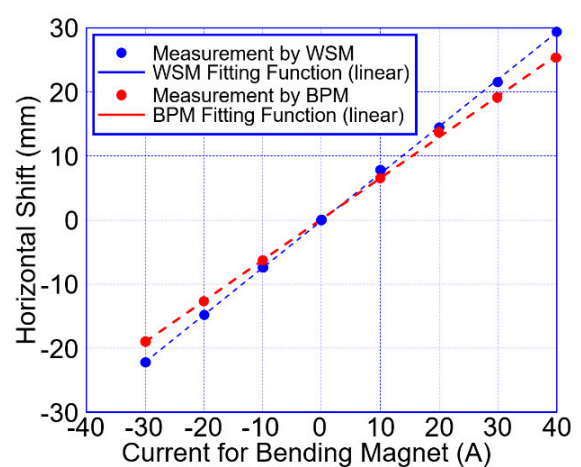


Figure 8. Beam position obtained by BPM and WSM.

beam displacements. In addition, we assumed a beam energy of 191 MeV, which corresponds to β of 0.56. The wire method is unsuitable for low- β beam fields, and errors can be found in the calibration. In the case of low- β fields, we must use the Equations (1) and (2) to fit these measurement data by considering the higher-order terms of the higher-harmonic number of the frequency (ω).

The relationship between the measured horizontal beam position and the current of the bending magnets was obtained. The BPM can be used for a beam position range of approximately 20 mm, and the WSM offset values were also obtained as well.

6. Conclusion

A diagnostic beam line was installed to measure the orbit displacement by using pairs of beam-bump magnets. Beam diagnostics, such as BPM and WSM, were designed and installed to observe horizontal beam displacement and its profile. We use both diagnostics to evaluate the beam displacement when separating H^- , H^0 and H^+ particles. In this paper, we have described the design of a wide-range BPM to extend the calibration function to a range of about 20.0 mm. A comparison of beam position measurements by BPM and WSM, revealed acceptable agreement between the two sets within a range of 20 mm, so both monitors can be utilized for large beam displacements. The newly developed BPM can perform online monitoring of the beam displacement without interrupting any operation. By constant, WSM cannot be used for online beam monitoring, but it can measure the beam orbit by performing horizontal scanning because of its high linearity over a wide aperture.

7. Acknowledgement

The authors would like to acknowledge the specialists who installed the diagnostics system arrangement, and performed the chicane test. The authors also appreciate the J-PARC writing support group, which continuously encouraged us to write this article.

References

- [1] Tamura J, Miura A, Morishita T, Ao H, Maruta T, Miyao T and Nemoto Y 2016 *Proc. LINAC16* (East-Lansing, MI, USA) MOPLR063
- [2] Miura A, Ouchi N, Oguri H, Hasegawa K, Miyao T and Ikegami M, 2015 *J. Korean Phys. Soc.*, **66** 3, pp 364-372
- [3] Shafer R E 1994 *AIP Conf. Proc.* **319** pp. 303
- [4] Forck P 2012 *Lecture Notes on Beam Instrumentation and Diagnostics*, (Text. of Joint Univ. Accelerator School) pp 9-39
- [5] Shafer R E 1985 *IEEE Trans. Nucl. Sci.* **32** pp 1933-37
- [6] Sato S, Igarashi Z, Lee S, Tomisawa T, Hiroki F, Kishiro J, Ikegami M, Kondo Y, Hasegawa K, Ueno A, Toyama T, Kamikubota N, Nigorikawa K, Tanaka M, Yoshikawa H 2004 *Proc. LINAC2004* (Lubeck, Germany) TUP70
- [7] Poisson Superfish Announcement by LANL Home Page: <http://laacg1.lanl.gov/laacg/>